Int. J. Electrochem. Sci., 13 **(2018)** 9600 – 9617, doi: 10.20964/2018.10.02

International Journal of
ELECTROCHEMICAL
SCIENCE
www.electrochemsci.org

Pantoprazole Sodium as a Corrosion Inhibitor for Zinc in Acidic Solutions

M. Saadawy

Chemistry Department, Faculty of Science, Alexandria University, Ibrahimia, P.O. box 426, Alexandria 21321
E-mail: marwan.saadawy@yahoo.com

Received: 26 February 2017 / *Accepted:* 9 January 2018 / *Published:* 1 September 2018

Pantoprazole Sodium (PAN) was tested as a corrosion inhibitor for zinc in aqueous solutions of 0.5M H_2SO_4, 1M HCl and 1M $HClO_4$ at 30^oC using absorbance measurement, electrochemical techniques; potentiodynamic polarization and AC-impedance techniques. The results obtained revealed that PAN could inhibit the corrosion of zinc effectively only in 1M $HClO_4$. The values of binding constants obtained for PAN in 0.5M H_2SO_4, 1M HCl and 1M $HClO_4$ solutions for zinc after fitting the data to different adsorption isotherms could be arranged as follows: perchloric acid > hydrochloric acid > sulphuric acid. This order agrees to a great extent with the values of inhibition efficiency calculated from absorbance and different electrochemical techniques.

Keywords: zinc; polarization; absorbance; AC-impedance; acid corrosion; inhibition; pantoprazole.

1. INTRODUCTION

Industrial processes usually involve the susceptibility of different metals and alloys to numerous types of corrosion as a consequence of aggressive attack by different corrosive reagents. Corrosion had a great interest of researchers in last decades because its occurrence causes the depletion of the world naturally-occurring resources of energy and materials which obliges the efficient exploitation of the contemporary materials and supreme preservation of metals and alloys. Acid wash processes are well-known industrial processes like acid cleaning, pickling, and scale-removal from metal surfaces [1]. Acid pickling is widespread utilized to get a clean metal surface free of scales or oxides which can be eliminated by several industrial processes like enameling, painting, galvanizing, cold rolling and electroplating. Addition of inhibitors is one of the methods used to reduce the rate of metal corrosion. A great attention is focused on zinc metal due to its important practical applications and uses; it is intensively used as a reactive anode during energy generation in electrochemical cells, in galvanization and in the case of corrosion under atmospheric conditions. In literature, several

compounds have been investigated as corrosion inhibitors for zinc in different aqueous solutions and a number of organic and inorganic compounds were reported to suppress the acid corrosion of zinc [2-12]. The hazards of most synthetic corrosion inhibitors motivated the use of green and environmentally-friendly compounds. Different researchers investigated the use of such green economic compounds for zinc [13-20]. Pantoprazole sodium can be used as a green corrosion inhibitor. This compound contains many π electrons and heteroatoms like sulfur, nitrogen, two fluorine atoms and four oxygen atoms, all of which are capable of achieving better adsorption of the molecule on the metal surface compared with other heterocyclic compounds [21]. Furthermore, Pantoprazole sodium has been reported [22] and more recently by Quraishi [23] to act as an efficient inhibitor for the acid corrosion of mild steel and also for copper [24]. The target of the current investigation is to test the inhibitory effect of pantoprazole sodium (PAN) as a benign drug on the acid corrosion of zinc in aqueous solutions of 0.5M H_2SO_4, 1M HCl and 1M $HClO_4$.

2. EXPERIMENTAL

2.1. Electrochemical Tests

Polarization and AC-impedance measurements were conducted using a frequency response analyzer Gill AC instrument. AC-impedance measurements were carried out using frequencies between 0.1 and $1x10^3$ Hz. The applied potential had signal amplitude of 10 mV around the rest potential. Scan rate of polarization experiments was 30 mV/min starting from cathodic potential (Ecorr - 250mV) going to anodic direction using a three electrode-mode cell. This wide range of potential permits the determination of Tafel slopes; β_a, β_c and estimation of corrosion current; i_{corr} by extrapolating the linear Tafel region to the corrosion potential. Reference and counter electrodes were saturated calomel electrode (SCE) and platinum sheet respectively. Rods of zinc were used for constructing the working electrodes. The chemical composition of these rods is presented in Table 1. Poly tetrafluoro ethylene (PTFE) rods were used for fixing the metal samples utilizing an epoxy resin in such a way that only one uncovered side of zinc rod surface will be exposed to solution. A long screw was fastened to the other end of zinc rod for electrical connection. The area of uncovered exposed part was approximately $1cm^2$ and was prepared for experiment by mechanical polishing using coarse emery papers followed by finer ones till reaching the finest grade of 1200. Double distilled water followed by A.R. ethanol was used to wash the samples thoroughly and finally rinsed with distilled water just before insertion into the cell. Each experiment was carried out with a newly polished electrode. Before polarization and AC-impedance measurements, the working electrode was introduced into the test solution and left for 10 min at the open circuit potential.

Table 1. Chemical analysis of the working electrode.

Element	**As**	**S**	**P**	**Pb**	**Fe**	**Zn**
wt%	0.00001	0.001	0.001	0.01	0.005	99.98

All the measurements were done in solutions thermostated at 30.0 ± 0.1^{o}C under unstirred conditions and open to the atmosphere. To test the reliability and reproducibility of the measurements, duplicate experiments were performed in each case of the same conditions.

2.2. Solution Preparation

The inhibitor, pantoprazole sodium (PAN) has the chemical structure, Figure 1, obtained from Beacon Pharmaceuticals Ltd. Chemicals Company. Stock solution of 0.01M PAN was prepared, then appropriate dilution is used to obtain different PAN concentrations inside the polarization cell. Analytical grade (Aldrich chemicals) concentrated acids, 98% H_2SO_4, 37% HCl, and 70% $HClO_4$ were used without further purification to prepare stock solutions of these acids with doubly distilled water then appropriate dilution is used to obtain 0.5M H_2SO_4, 1M HCl, and 1M $HClO_4$ inside the polarization cell.

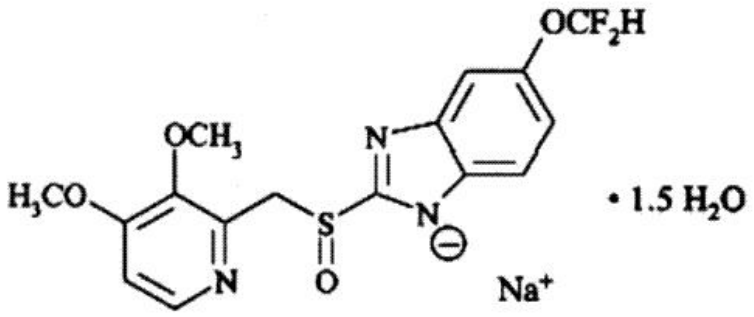

Figure 1. Structure of pantoprazole sodium (PAN)
IUPAC name: (RS)-6-(Difluoromethoxy)-2-[(3,4-dimethoxypyridin-2-yl)methylsulfinyl]-1H-benzo[d] imidazole.

2.3. Absorbance measurement

Concentrations of zinc ion and dissolved oxygen, $O_{2,diss}$ were determined by measuring the absorbance of solutions of 0.5M H_2SO_4, 1M HCl or 1M $HClO_4$ containing different concentrations of PAN in presence of 10^{-3}M Zn^{+2} using Hach spectrophotometer DR 2010 [25] and adjusting the wavelength in the range of 200-400 nm. The blanks were taken as the pure acid solutions containing 10^{-3}M Zn^{+2} in absence of PAN.

3. RESULTS AND DISCUSSION

3.1. Potentiodynamic Polarization Results

Figures (2-4) show the potentiodynamic polarization curves for zinc dissolution in aqueous solutions of 0.5 M H_2SO_4, 1M HCl and 1M $HClO_4$ respectively in the absence and presence of different concentrations of pantoprazole sodium (PAN) at 30°C. Figure 2 indicates that the addition of PAN affects both anodic and cathodic parts of the polarization curves indicating that PAN acts as mixed-type inhibitor for zinc in 0.5M H_2SO_4 solution i.e. retards the zinc dissolution reaction and

hydrogen evolution reactions. Figures 3,4 indicate that only cathodic part of the polarization curves are affected by the addition of PAN indicating that PAN is classified as cathodic-type inhibitor for zinc in 1M HCl and 1M $HClO_4$ i.e. the corrosion inhibition of zinc takes place by retarding the hydrogen evolution reaction.

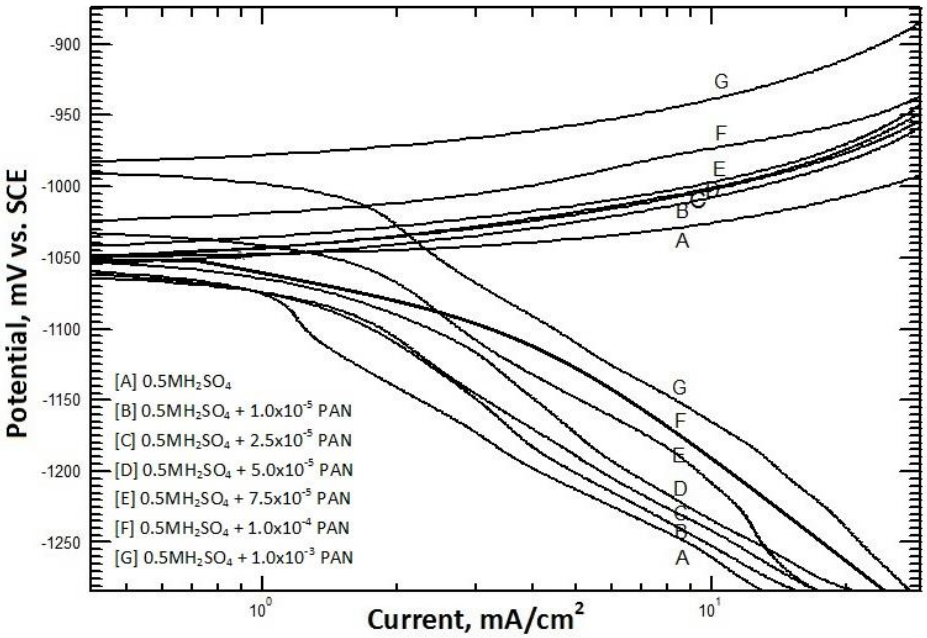

Figure 2. Potentiodynamic polarization curves for zinc in 0.5 M H_2SO_4 , in the absence and presence of different concentrations of PAN at 30°C.

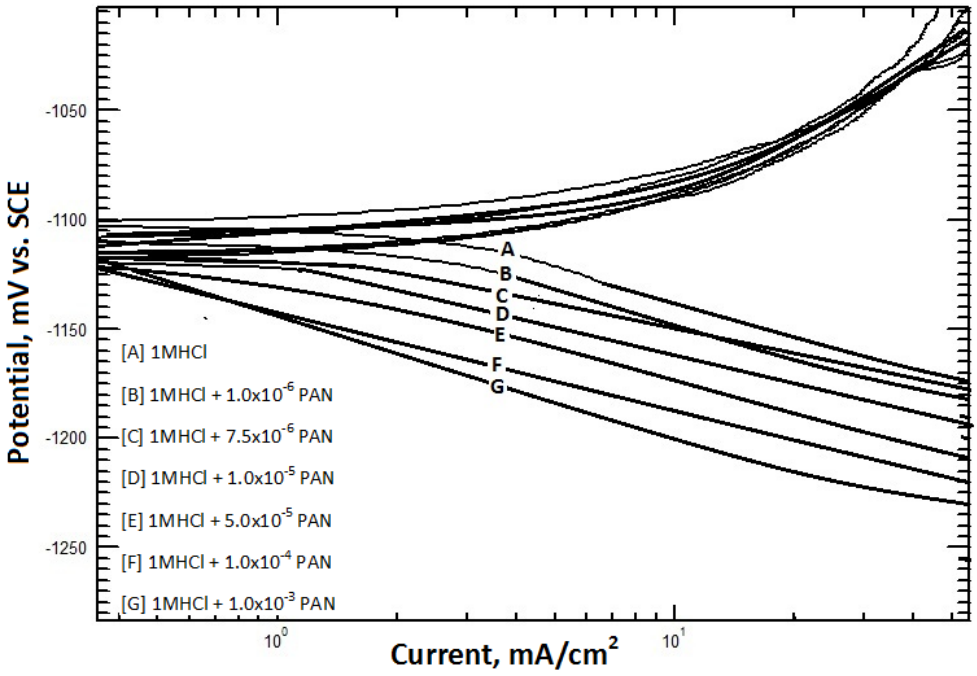

Figure 3. Potentiodynamic polarization curves for zinc in 1M HCl, in the absence and presence of different concentrations of PAN at 30°C.

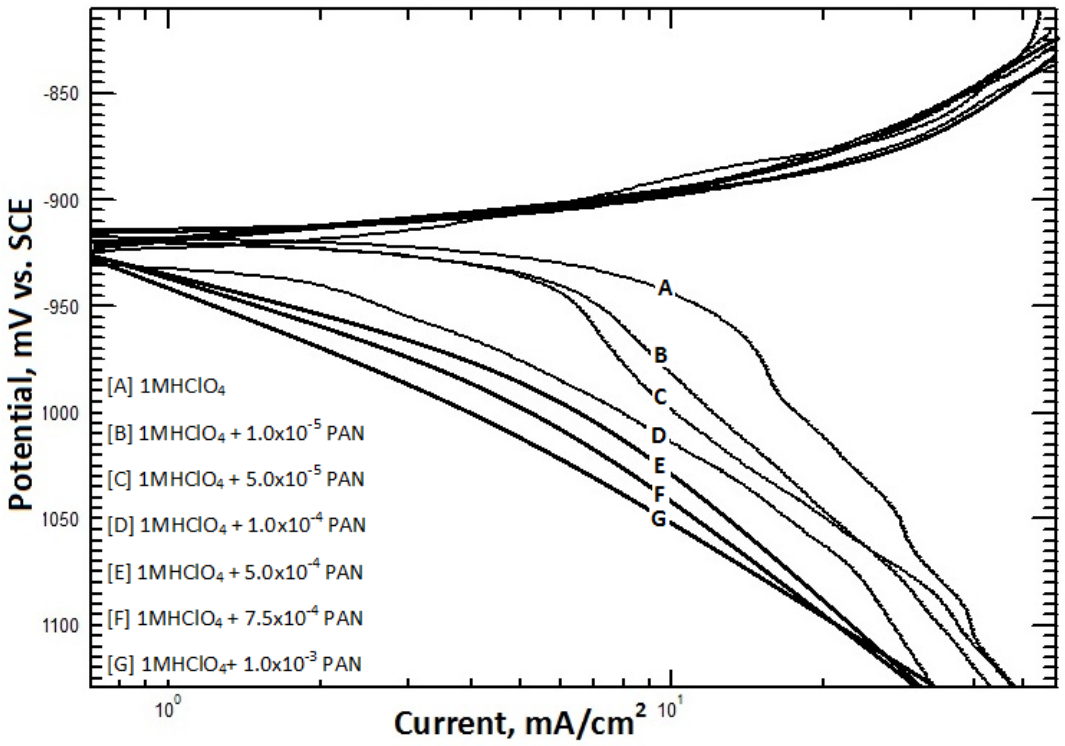

Figure 4. Potentiodynamic polarization curves for zinc in 1M $HClO_4$, in the absence and presence of different concentrations of PAN at 30°C.

The values of the electrochemical polarization parameters: corrosion potential; E_{corr} , anodic and cathodic Tafel slopes; β_a, β_c and corrosion current density; i_{corr} for the dissolution of zinc in 0.5 M H_2SO_4, 1M HCl and 1M $HClO_4$ at 30°C in the absence and presence of different concentrations of PAN are given in Tables (2-4).

Table 2. The electrochemical polarization parameters of zinc dissolution in 0.5 M H_2SO_4, in the absence and presence of different concentrations of PAN at 30°C.

Conc., mol. L^{-1}	Electrochemical parameters				
	- E_{corr} (mV vs. SCE)	β_a (mV.decade^{-1})	$-\beta_c$ (mV.decade^{-1})	i_{corr} (mA.cm^{-2})	% inh
0.00	1055	118.7	173.1	2.00	-
$1.0x10^{-5}$	1050	108.9	199.5	1.65	17.5
$2.5x10^{-5}$	1045	96.9	203.5	1.49	25.5
$5.0x10^{-5}$	1040	120.1	201.3	1.44	28.0
$7.5x10^{-5}$	1030	110.6	176.5	1.36	32.0
$1.0x10^{-4}$	1020	120.2	167.9	1.31	34.5
$2.5x10^{-4}$	1015	125.1	151.3	1.28	36.0
$5.0x10^{-4}$	1010	124.9	158.5	1.27	36.5
$7.5x10^{-4}$	995	129.4	156.2	1.25	37.5
$1.0x10^{-3}$	975	105.3	195.3	1.23	38.5

Table 3. The electrochemical polarization parameters of zinc dissolution in 1M HCl, in the absence and presence of different concentrations of PAN at 30°C.

Conc., mol. L^{-1}	Electrochemical parameters				
	$-E_{corr}$ (mV vs. SCE)	β_a (mV.decade^{-1})	$-\beta_c$ (mV.decade^{-1})	i_{corr} (mA.cm^{-2})	% inh
0.00	1103	79	87	2.60	---
$1.0x10^{-6}$	1108	89	84	2.40	7.7
$5.0x10^{-6}$	1110	113	97	2.34	10.0
$7.5x10^{-6}$	1112	92	83	2.31	11.1
$8.0x10^{-6}$	1113	75	87	2.26	13.1
$1.0x10^{-5}$	1115	112	104	2.10	19.2
$5.0x10^{-5}$	1117	90	84	1.95	25.0
$1.0x10^{-4}$	1118	93	109	1.80	30.7
$5.0x10^{-4}$	1119	82	91	1.58	39.2
$1.0x10^{-3}$	1118	101	102	1.52	41.5

Table 4. The electrochemical polarization parameters of zinc dissolution in 1M $HClO_4$, in the absence and presence of different concentrations of PAN at 30°C.

Conc., mol. L^{-1}	Electrochemical parameters				
	$-E_{corr}$ (mV vs. SCE)	β_a (mV.decade^{-1})	$-\beta_c$ (mV.decade^{-1})	i_{corr} (mA.cm^{-2})	% inh
0.00	922	115	226	14.51	---
$1.0x10^{-5}$	930	126	241	12.30	15.2
$4.0x10^{-5}$	936	143	235	10.11	30.3
$5.0x10^{-5}$	955	175	244	8.18	43.6
$6.0x10^{-5}$	965	120	270	6.50	55.2
$7.0x10^{-5}$	959	140	243	4.99	65.6
$8.0x10^{-5}$	964	147	271	3.76	74.1
$1.0x10^{-4}$	935	119	265	3.18	78.1
$1.5x10^{-4}$	955	121	228	2.88	80.1
$2.5x10^{-4}$	969	120	241	2.44	83.2
$5.0x10^{-4}$	940	139	249	2.22	84.7
$7.5x10^{-4}$	953	132	251	1.97	86.4
$1.0x10^{-3}$	933	128	261	1.15	92.1
$1.5x10^{-3}$	942	134	252	0.82	94.3

Tables 2-4 illustrate that introducing this compound to the acid solutions has no appreciable effect on the corrosion potential (E_{corr}) accompanied with a decrease of the values of corrosion current density (i_{corr}) showing that it could be classified as pickling inhibitor [26]. Inhibitive effect of PAN was estimated by calculating its inhibition efficiency (% inh) from polarization experiments using the following equation [24]:

$$\% \text{ inh} = [(i_o - i) / i_o] \text{ x}100 \quad (1)$$

Where i_o and i are the corrosion current densities without and with the addition of PAN respectively. Slight variations of anodic and cathodic Tafel slopes, β_a and β_c confirm that the mechanism of corrosion reaction is not altered by increasing the concentration of this compound [27]. This confirms the adsorption action of PAN at both anodic and cathodic areas in case of sulphuric acid and thus reducing the tendency of anodic and cathodic reactions [28,29] or by adsorption only at local cathodic sites in case of hydrochloric or perchloric acid solutions. Moreover, at cathodic areas, the combination of the adsorbed hydrogen atoms to form hydrogen gas molecules would be affected by the steric hindrance of the adsorbed molecules and thus inhibiting the cathodic reaction in case of hydrochloric or perchloric acids and upon increasing the inhibitor concentration, more inhibitor molecules would be adsorbed by virtue of van der Waals interaction forces among inhibitor molecules. Thus increasingly, close-packed film will be growing and causing segregation of the metal surface from the solution.

3.2. Absorbance Measurement

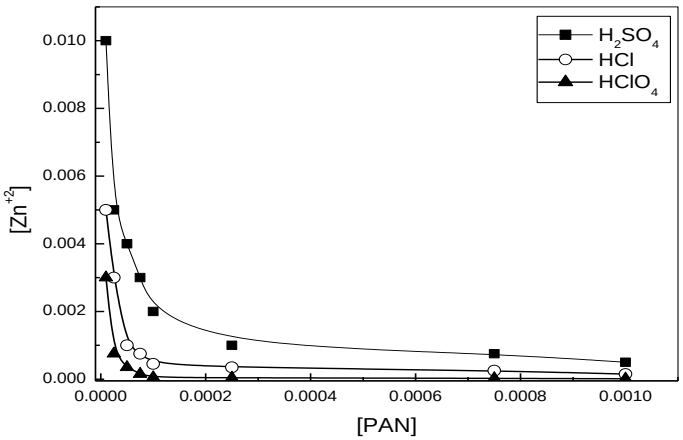

Figure 5. Variation of concentration of Zn^{+2} in 0.5M H_2SO_4, 1M HCl and 1M $HClO_4$ with the concentration of PAN.

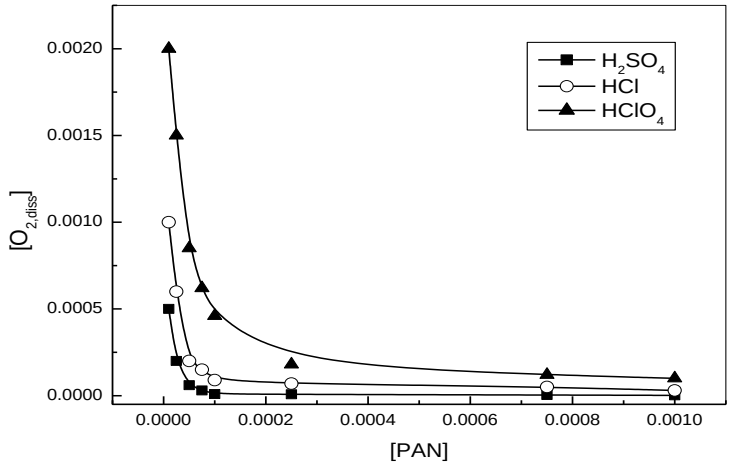

Figure 6. Variation of concentration of dissolved oxygen $O_{2,diss}$ in 0.5M H_2SO_4, 1M HCl and 1M $HClO_4$ with the concentration of PAN.

Figure 5 demonstrates the variation of concentration of Zn^{+2} in aqueous solutions of 0.5 M H_2SO_4, 1M HCl and 1M $HClO_4$ with the concentration of PAN. It is evident that the increase of PAN concentration is accompanied with the decrease of Zn^{+2} concentration in all acid solutions confirming that PAN suppresses the anodic dissolution of zinc. Perchloric acid solution has a minimum concentration of Zn^{+2} where PAN has maximum inhibitive action.

Figure 6 demonstrates the change of concentration of dissolved oxygen $O_{2,diss}$ in aqueous solutions of 0.5 M H_2SO_4, 1M HCl and 1M $HClO_4$ with the concentration of PAN. It is evident that the increase of PAN concentration is accompanied with the increase of $O_{2,diss}$ concentration confirming that PAN suppresses the oxygen reduction reaction. Perchloric acid has a maximum concentration of $O_{2,diss}$.

3.3. Electrochemical Impedance Spectroscopy Results:

Impedance measurements were achieved at 30°C to test the effect of this compound on the kinetics of zinc corrosion in acid solutions. Figures (7-9) demonstrate the Nyquist plots of zinc in aqueous solutions of 0.5 M H_2SO_4, 1M HCl, and 1M $HClO_4$ in the absence and presence of different concentrations of PAN at 30°C.

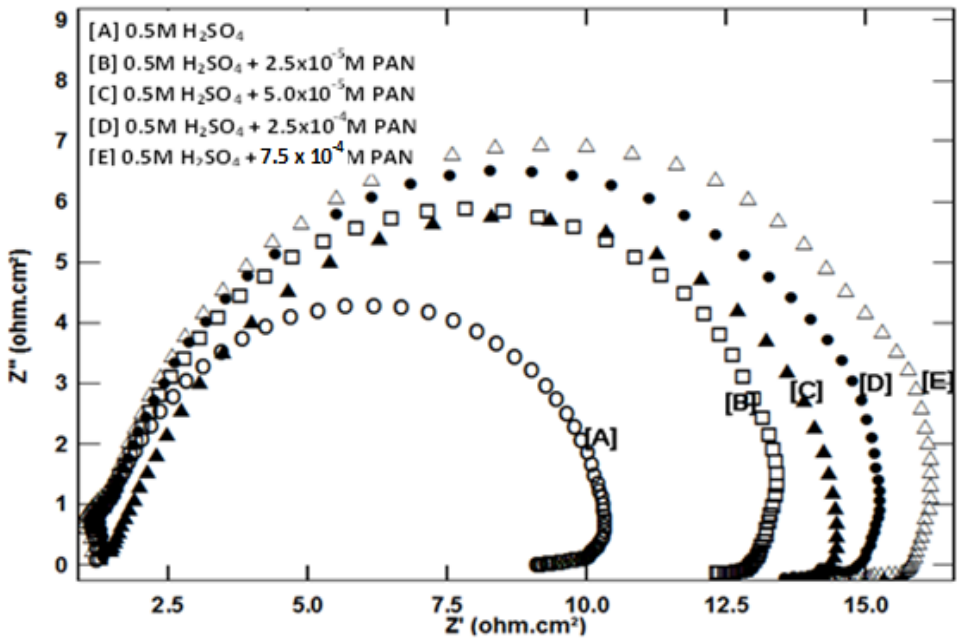

Figure 7. Nyquist plots for zinc in 0.5 M H_2SO_4, in the absence and presence of different concentrations of PAN at 30°C.

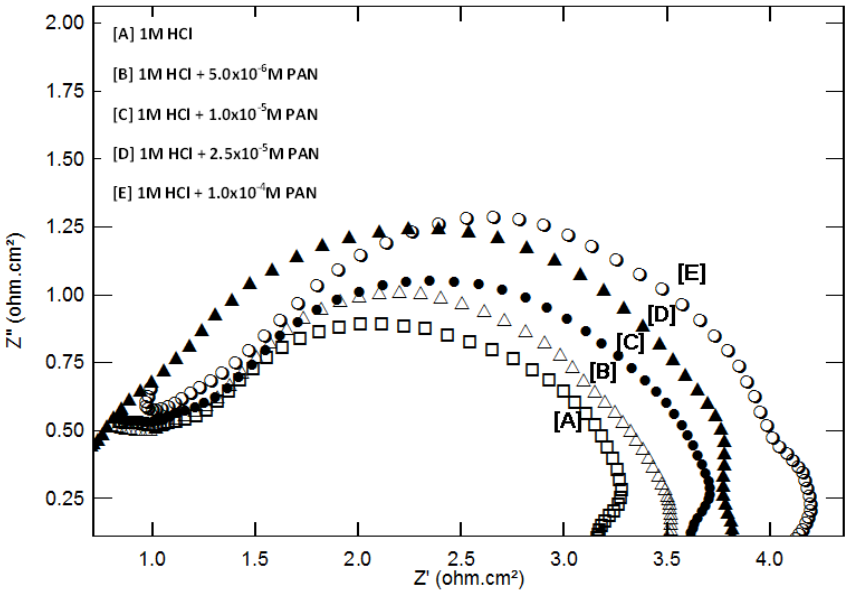

Figure 8. Nyquist plots for zinc in 1M HCl, in the absence and presence of different concentrations of PAN at 30°C.

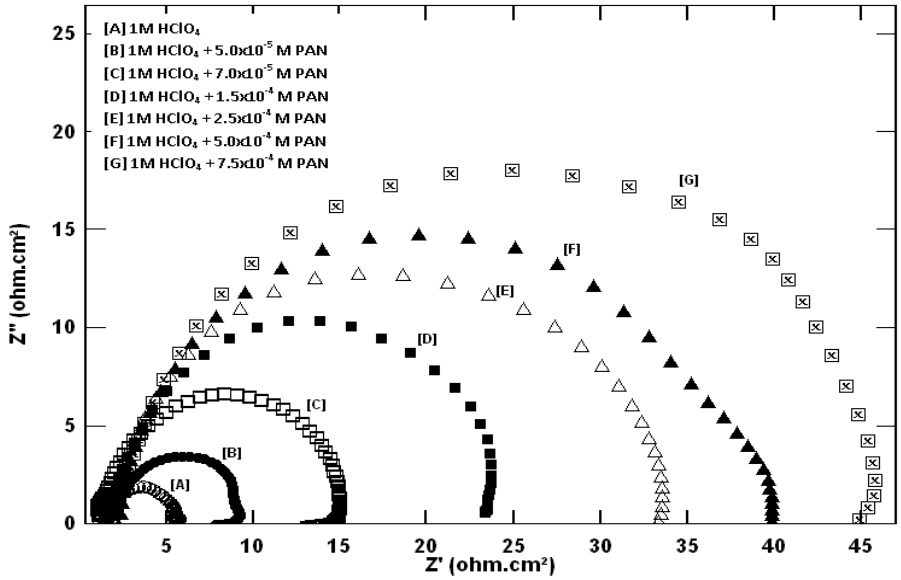

Figure 9. Nyquist plots for zinc in 1M $HClO_4$, in the absence and presence of different concentrations of PAN at 30°C.

These plots have the appearance of depressed semicircles revealing that zinc dissolution is activation-controlled process so it is concluded that the mechanism of zinc corrosion is not changed by the addition of this compound to the acid solution [30]. Moreover, it is evident that the size of the depressed semicircles is directly proportional to the concentration of PAN. Corrosion inhibition generally depends on several factors like the surface charge of metal, the acid bath concentration, bulk solution temperature and time of adsorption [31]. Moreover, the adsorption process depends on some parameters related to the inhibitor like its concentration, its molecular size, number of its adsorption

centres, the charge density on each adsorption centre, its basicity and its ability to form metallic complexes. The depression in Nyquist semicircles is characteristic for solid electrodes and often attributed to frequency inhomogeneity of the solid electrode [32]. A constant phase element (CPE) is used to describe the frequency-independent phase shift which exists between the applied AC potential and its current response, CPE is defined in impedance representation as in equation (2).

$$Z_{CPE} = Q^{-1} (j\omega)^{-n} \quad (2)$$

Where Q is the CPE constant, ω is the angular frequency (rad.s^{-1}), j^2= -1; is the imaginary number and n is a CPE exponent which can be used as a gauge for the heterogeneity or roughness of the surface [33]. Depending on the value of n, CPE can represent capacitance (n = 1, Q = C). C_{dl} values are derived from CPE parameters according to equation (3).

$$C_{dl=}(Q.R_{ct}^{1-n})^{1/n} \quad (3)$$

Where R_{ct} is the charge transfer resistance which is inversely proportional to the corrosion rate. Figure 10 illustrates the electrical equivalent circuit employed to analyse the impedance spectra. This Figure included the solution resistance; R_s, the charge transfer resistance; R_{ct} that measure the electron transfer across the surface and the double layer capacitance; C_{dl} of zinc.

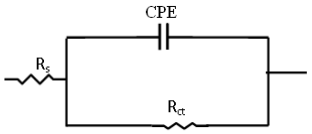

Figure 10. The electrochemical equivalent circuit used to fit the impedance measurements for zinc in aqueous acidic solutions.

Table 5. The electrochemical impedance parameters for zinc dissolution in 0.5M H_2SO_4, in the absence and presence of different concentrations of PAN at 30 ºC.

Conc., mol. L^{-1}	**Impedance parameters**			
	R_s Ohm.cm^2	**C_{dl} µF.cm^{-2}**	**R_{ct} Ohm.cm^2**	**% inh**
0.00	1.17	69.2	9.3	-
$1.0x10^{-5}$	1.81	67.5	11.6	19.8
$2.5x10^{-5}$	1.31	59.8	12.8	27.3
$5.0x10^{-5}$	1.44	56.2	13.5	31.1
$7.5x10^{-5}$	1.27	54.1	14.4	35.4
$1.0x10^{-4}$	0.79	53.9	14.7	35.8
$2.5x10^{-4}$	1.27	52.7	14.9	36.1
$5.0x10^{-4}$	1.51	49.4	15.3	36.8
$7.5x10^{-4}$	0.82	45.3	15.8	37.2
$1.0x10^{-3}$	0.89	40.2	16.2	37.3

Table 6. The electrochemical impedance parameters of zinc dissolution in 1M HCl, in the absence and presence of different concentrations of PAN at 30°C.

Conc., mol. L^{-1}	Impedance parameters			
	R_s Ohm.cm^2	C_{dl} µF.cm^{-2}	R_{ct} Ohm.cm^2	% inh
0.00	0.64	350	2.41	-
$1.0x10^{-6}$	1.33	321	2.61	7.5
$5.0x10^{-6}$	1.09	340	2.63	8.3
$7.5x10^{-6}$	1.10	311	2.67	9.8
$8.0x10^{-6}$	1.00	292	2.71	11.2
$1.0x10^{-5}$	0.98	275	2.85	15.4
$5.0x10^{-5}$	0.89	241	3.19	24.5
$1.0x10^{-4}$	1.02	220	3.43	31.8
$5.0x10^{-4}$	1.05	188	3.60	37.4
$1.0x10^{-3}$	0.91	160	3.92	38.5

Table 7. The electrochemical impedance parameters of zinc dissolution in 1M $HClO_4$, in the absence and presence of different concentrations of PAN at 30°C.

Conc., mol. L^{-1}	Impedance parameters			
	R_s Ohm.cm^2	C_{dl} µF.cm^{-2}	R_{ct} Ohm.cm^2	% inh
0.00	1.1	205	4.5	---
$4.0x10^{-5}$	1.2	118	6.9	34.8
$5.0x10^{-5}$	1.7	89	8.6	47.7
$6.0x10^{-5}$	0.6	71	11.1	59.4
$7.0x10^{-5}$	1.1	63	14.9	69.8
$8.0x10^{-5}$	1.5	58	20.8	78.4
$1.0x10^{-4}$	0.6	49	22.1	79.6
$1.5x10^{-4}$	1.5	39	24.2	81.4
$2.5x10^{-4}$	1.5	32	33.5	86.6
$5.0x10^{-4}$	1.9	28	37.1	87.9
$7.5x10^{-4}$	1.8	24	45.7	90.1
$1.0x10^{-3}$	1.0	20	58.2	92.2
$1.5x10^{-3}$	1.0	8	71.0	93.7

Excellent fit with this model was obtained for all experimental data and the fit results for zinc in aqueous solution of 0.5M H_2SO_4, 1M HCl and 1M $HClO_4$ in the absence and presence of different concentrations of the inhibitor at 30°C are presented in Tables (5-7).

The data show that increasing the concentration of PAN have led to increasing the charge transfer resistance that was accompanied with decreasing the double layer capacitance which could be ascribed to the adsorption of this compound over zinc surface [34].

The inhibition efficiency (% inh) of PAN was calculated from impedance measurements by applying the following relationship [24]:

$$\% \text{ inh} = [(R_{ct} - R_{cto}) / R_{ct}] \text{ x}100 \quad (4)$$

Where R_{ct} and R_{cto} are charge transfer resistances with and without the addition of the inhibitor, respectively.

3.4. Application of the Adsorption Isotherms:

The action of an inhibitor in acidic media is attributed to its adsorption [35] at the metal/solution interface. This phenomenon could occur through (i) electrostatic attraction between the charged metal and inhibitor molecules (ii) dipole-type interaction between unshared electron pairs of the inhibitor with the metal (iii) π-interaction with the metal, and (iv) a combination of all of the above [36]. The inhibition action was considered as simple substitution process [37], in which an inhibitor molecule displaces an x number of water molecules adsorbed on the metal surface, viz.

$$I_{(aq)} + x(H_2O)_{sur} \rightarrow I_{(Sur)} + x(H_2O)_{aq} \quad (5)$$

Where x is the number of adsorbed water molecules displaced by one inhibitor molecule. The degree of surface coverage (θ) of the metal surface by adsorbed PAN molecules was calculated from impedance measurements using the equation (6):

$$\theta = (R_{ct} - R_{cto})/R_{ct} \quad (6)$$

The variations of surface coverage of PAN with its concentration in the three different acid solutions are shown in Figure 11.

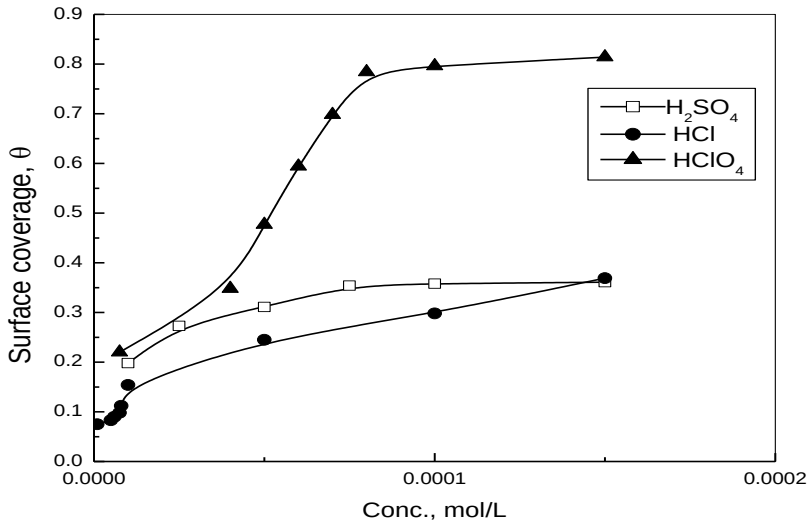

Figure 11. Variation of surface coverage calculated from impedance measurements with the concentration of PAN for zinc in different acid solutions.

Adsorption isotherms present in Figure 11 are characterized by an initial sharply-rising part indicating the establishment of a mono-layer adsorbate films on zinc. At high concentrations, the inhibition efficiency was nearly constant indicating complete saturation of the surface by the inhibitor molecules. The determination of the type of adsorption isotherm that fits the data of PAN at the zinc/solution interface gives very important information about the adsorption process.

Langmuir, Flory Huggins isotherms and Kinetic-Thermodynamic model were used to fit the corrosion data of PAN.

The Langmuir isotherm is given by [38]

$$[\theta /(1- \theta)]=KC \quad (7)$$

Where K is the binding constant representing the interaction of the additives with the metal surface and C is the concentration of the additives.

Flory-Huggins isotherm is given by [39]

$$\theta / [x(1- \theta)^x] = KC \quad (8)$$

Where x is the size parameter; is a measure of the number of adsorbed water molecules displaced by a given inhibitor molecule. Kinetic-Thermodynamic model is given by [40]

$$\log [\theta / (1- \theta)] = \log K' + y \log C \quad (9)$$

Where y is the number of inhibitor molecules occupying one active site. The binding constant; K is given by:

$$K = K' (1/y) \quad (10)$$

Figure 12 shows the application of Langmuir model to the results of adsorption of PAN on zinc surface in different acid solutions.

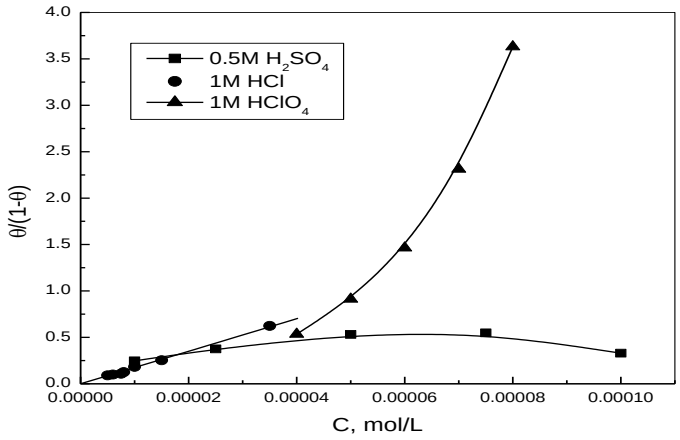

Figure 12. Linear fitting of the data of PAN for zinc in different acid solutions to Langmuir isotherm

Figure 12 illustrates the presence of non-ideal behaviour in the adsorption process [26] of PAN on zinc surface since Langmuir isotherm is not applicable to fit the data of the compound in sulphuric and perchloric acids solutions, however, Langmuir isotherm is applicable to fit the data of its adsorption in hydrochloric acid solution confirming its ideal behaviour in presence of 1M HCl. Figure 13 shows the application of Flory-Huggins model to fit the adsorption data of PAN on zinc surface in different acid solutions.

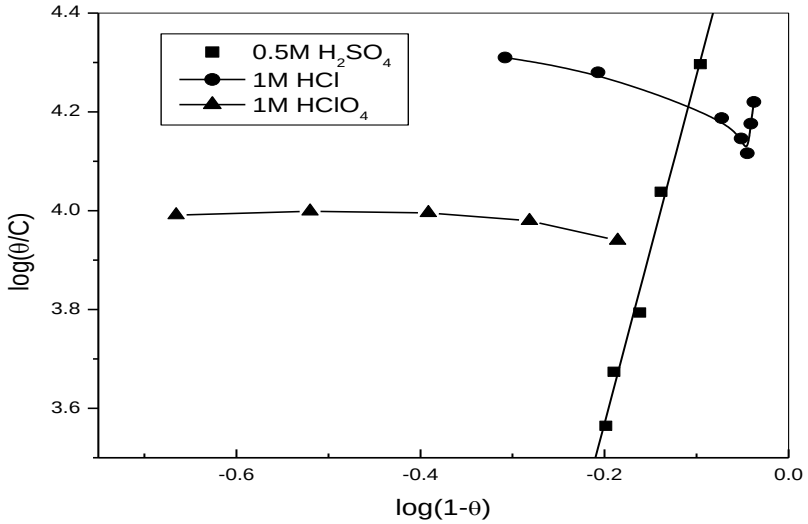

Figure 13. Linear fitting of the data of PAN for zinc in different acid solutions to Flory Huggins isotherm.

Figure 14 shows the application of Kinetic-Thermodynamic model to fit the adsorption data of PAN on zinc surface in different acid solutions.

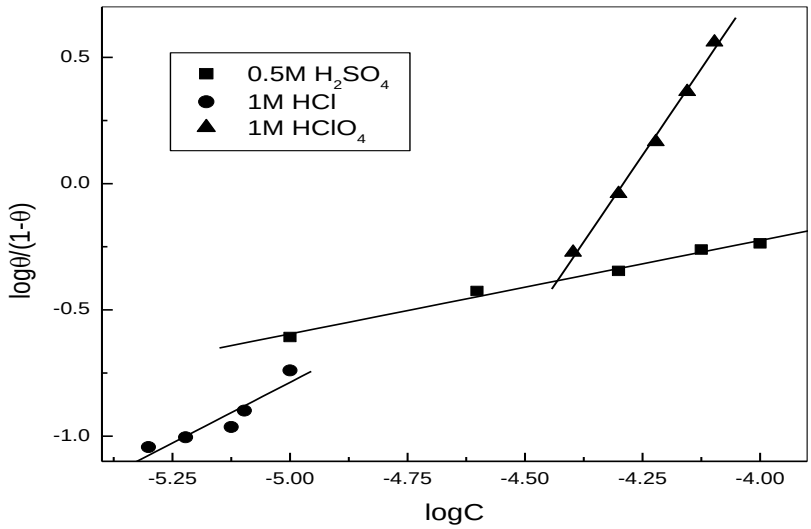

Figure 14. Linear fitting of the data of PAN for zinc in different acid solutions to Kinetic-Thermodynamic isotherm model.

The parameters obtained from the application of last models are depicted in Table 8.
It is clear from Table 8 that Flory-Huggins isotherm is not applicable to the data of the inhibitor in hydrochloric acid and perchloric acid solutions but applicable in sulphuric acid solution. As shown in Table 8, the value of the size parameter x indicates that in H_2SO_4, the adsorbed PAN molecule displaces more than one water molecule from the zinc surface [41] .

Kinetic-Thermodynamic model is also found to fit the data of the inhibitor. The values of 1/y obtained from Kinetic-Thermodynamic model indicates that PAN displaces more than one water molecule in sulphuric acid and only one molecule in hydrochloric acid while multilayer adsorption occurs in case of perchloric acid. The binding constant; K value obtained from Flory-Huggins isotherm was in a good agreement to that obtained from Kinetic-thermodynamic model. Large values of K mean better inhibition efficiency of a given compound, i.e., stronger electrical interaction between the double layer existing at the phase boundary and the adsorbing molecules. Small values of K, however comprise those interactions by adsorbing molecules and the metal surface are weaker, denoting that the molecules are easily removable by the solvent molecules from the surface [42].

Table 8. Linear fitting parameters of PAN for zinc in different acids according to the applied models.

Model parameters					
Acid medium	Langmuir	Flory-Huggins		Kinetic-Thermodynamic	
	K	X	K	1/y	K
Sulphuric acid	--	6.95	$8x10^3$	3.0	$3.5 x10^3$
Hydrochloric acid	$1.6x10^4$	--	--	1.04	$1.5 x10^4$
Perchloric acid	--	--	--	0.40	$5.5 x10^4$

Hence, according to the numerical values of K obtained, the inhibition efficiency of the compound in the three acids could be arranged in the order:

Perchloric acid > Hydrochloric acid > Sulphuric acid

This order agrees to a great extent with the values of inhibition efficiency calculated from absorbance graphs (Figures 5,6), polarization results (Tables 2-4) and impedance results (Tables 5-7), accordingly, Mechanism of inhibition is suggested to be attributed to adsorption of PAN on zinc surface followed by film formation that reduces the available active area exposed to acid attack.

3.5. Effect of Exposure Time

It has been reported [43] that exposure time of metal in aggressive solutions affects greatly the inhibition capability of organic compounds. The effect of exposure time on the corrosion behaviour of zinc in 1M $HClO_4$ solution after the addition of 10^{-3}M PAN was studied using AC-impedance technique to prove its inhibition stability with time. Figures 15 shows the Nyquist plots for zinc immersed in 1M $HClO_4$ in presence of 10^{-3}M PAN during different immersion times.

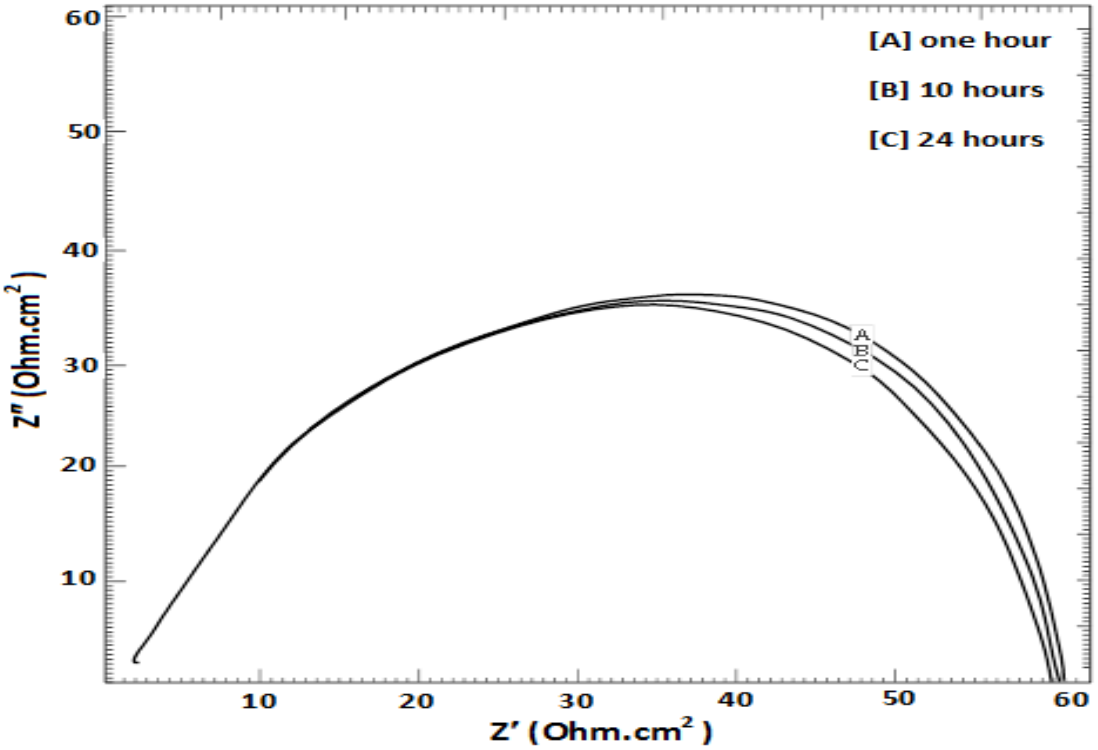

Figure 15. Nyquist plots for zinc immersed in 0.5 M H_2SO_4 in presence of 10^{-3}M PAN after different immersion times.

It can be noticed from Figure 15 that the inhibition efficiency of PAN for zinc corrosion is nearly constant after 24 hours of exposure to 1M $HClO_4$ confirming that the ability of PAN to suppress zinc corrosion persists with time.

4. CONCLUSIONS

The main conclusions obtained from this study are:

● PAN can be used as an effective corrosion inhibitor for zinc in 1M $HClO_4$.

● Potentiodynamic polarization results have shown that PAN acts as mixed-type inhibitor for zinc in 0.5M H_2SO_4 and cathodic-type inhibitor for zinc in 1M HCl and 1M $HClO_4$.

● AC-impedance measurements showed that in the three acid solutions, the addition of this compound does not alter the mechanism of zinc dissolution and is being controlled by the rate of the charge transfer process across the phase boundary in the uninhibited and inhibited acid solutions.

● The order of inhibition efficiency of PAN for zinc in the three acids is:

Perchloric acid > Hydrochloric acid > Sulphuric acid

ACKNOWLEDGEMENTS
The author wishes to thank Prof. Dr. Beshir Ahmed Abd El-Nabey, Prof. Dr. Essam Khamis and Prof. Dr. Ashraf Moustafa, Department of chemistry, Faculty of Science, Alexandria University, Alexandria, Egypt for continuous support and providing advanced instruments.

References

1. G. Schmitt, *Br. Corrosion*, 19 (1984) 165.
2. Lin Wang, Jian-Xin Pu and Hui-Chun Luo, *Corros. Sci*., 45 (2003) 677.
3. Y. Ein-Eli, M. Auinat and D. Starovetsky, *J. Power Sources*, 114 (2003) 330.
4. K. Aramaki, Corros. Sci., 43 (2001) 1985.
5. Y.K. Agrawal, J.D. Talati, M.D. Shah, M.N. Desai and N.K. Shah, *Corros. Sci.*, 46 (2004) 633.
6. J.D. Talati, M.N. Desai and N.K. Shah, *Mater. Chem. Phys*., 93 (2005) 54.
7. S. M. Ali and H. A. Al Lehaibi, *Transactions of Nonferrous Metals Society of China*, 26 (2016) 3034.
8. C.N. Panagopoulos, E.P. Georgiou and C. Markopoulos, *Corros. Sci.*, 70 (2013) 62.
9. R. T. Vashi and H. M. Bhajiwala, *Depharma Chemica*, 2 (2010) 272.
10. M. Abdallah, I.A. Zaafarany and B.A. AL Jahdaly, *J. Mater. Environ. Sci*., 7 (2016) 1107.
11. V.I. Vigdorovich, A.N. Zavershinskii, L.E. Tsygankova, T.N. Nazina, M.N. Esina and N.V. Shel, *International journal of corrosion and scale inhibition*, 6 (2017) 1.
12. A.I. Ali, H.E. Megahed, M.A. El-Etre and M.N. Ismail, *J. Mater.Environ.Sci*., 5 (2014) 923.
13. A.A. El Hosary, R.M. Saleh and A.M. Shams El Din, *Corros. Sci*., 12 (1972) 897.
14. A.A. El Hosary and R.M. Saleh, *Corrosion*, 2 (1993) 911.
15. A. M. Abdel-Gaber, *Int. J. Appl. Chem*., 3 (2007) 161.
16. A.Y. El-Etre, M. Abdallah and Z.E. El-Tantawy, *Corros. Sci*., 47 (2005) 385.
17. E.E. Foad El-Sherbini, S.M. Abdel Wahaab and M. Deyab, *Mater. Chem. Phys*., 89 (2005) 183.
18. Olusegun K. Abiola and A.O. James, *Corros. Sci*., 52 (2010) 661.
19. M.S. Morad, *J. Appl. Electrochem*., 29 (1999) 619.
20. M. Abdallah, *Corros. Sci*., 45 (2003) 2705.
21. M. Mahdavian and S. Ashhari, *Electrochim. Acta* 55 (2010) 1720.
22. A. Espinoza-Vázquez, G. E. Negrón-Silva, D. Ángeles-Beltrán, M. Palomar-Pardavé, M. Romero-Romo and H. Herrera-Hernández, *Electrochem. Soc. Transactions*, 36 (2011) 207.
23. Sudheer and M. A. Quraishi, *Arab. J. Sci. Eng.*, 38 (2013) 99.
24. M. Saadawy, *Arab. J. Sci. Eng*., 41 (2016) 177.
25. WWW.DR 2010 Spectrophotometer Instrument User Manual - Hach.com
26. G. Lyberatos and L. Kobotiatis, *Corrosion*, 47 (1991) 820.
27. B.G. Ateya, B.E. El-Anadouli, F.M.A. El-Nizamy, *Bull. Chem. Soc*., 54 (1981) 3157.
28. P. Hoar and R. D. Holliday, *J. Appl. Chem*., 3 (1953)502.
29. N. Hackerman and J. D. Sudbury, *Ind. Electrochem. Soc*., 97 (1950) 109.
30. Z. Szklaraska, Smialowska, "Electrochemical and Optical Techniques for Studying of Metallic Corrosion" (1991).
31. H.B. Rudresh and S. M. Mayanna, *Surf. Technol*., 6 (1977) 139.
32. A. Popova and M. Christova, *Corros. Sci* ., 48 (2006) 3208.
33. D.A. Lopez, S.N. Simison and S.R. De Sanchez, *Electrochim. Acta*., 48 (2003) 485.
34. K. Aramaki, M. Hagiwara and H. Nishihara, *Corros. Sci*., 5 (1987) 487.
35. K. Aramaki, Y. Node and H. Nishihara, *J. Electrochem. Soc*., 137 (1990) 1354.
36. D. Schweinsberg, G. George, A. Nanayakkawa and D. Steinert, *Corros. Sci*., 28 (1988) 33.
37. B. Ateya, B. El-Anadouli, F. El-Nizamy, *Corros. Sci.*, 24 (1984) 509.
38. I. Langmuir, *J. Am. Chem. Soc*., 38 (1916) 2221.

39. P. J. Florry, *J. Chem. Phys*., 10 (1942) 51.
40. A.A. El-Awady, B.A. Abd-El-Nabey, S.G. Aziz, *J. Electrochem. Soc*., 19 (1992) 2149.
41. B.A. Abd-El-Nabey, E-Kamis, M.Sh. Ramadan, A. El-Gindy, *Corrosion*, 52 (1996) 671.
42. N. Khalil, F. Mahgoub, B.A. Abd-El-Nabey, A. Abdel-Aziz, *CEST*, 38(2003) 205.
43. M. Palomar-Pardavé, M. Romero-Romo, H. Herrera-Hernandez, M.A. Abreu-Quijano,Natalya V. Likhanova, J. Uruchurtu, and J.M. Jurez-Garcia, *Corros. Sci*., 54 (2012) 231.